JOURNAL OF APPLIED POLYMER SCIENCE VOL. 20, 315–325 (1976)

# A Comparison of Drag Reduction for Flows in Circular Tubes with Flow Between Parallel Planes

D. B. CLARK and F. RODRIGUEZ, *School of Chemical Engineering, Olin Hall, Cornell University, Ithaca, New York 14853*

## Synopsis

Drag reduction in the turbulent flow of aqueous solutions of polyacrylamide and poly(ethylene oxide) was studied in tubes and parallel plates. Friction factors were determined at Reynolds numbers up to 20,000 for polymer concentrations of 0.10 to 400 g/m$^3$ in glass tubes run in a constant-head, gravity flow system in which the velocity was determined from the horizontal distance traveled by the effluent stream while falling a set vertical distance; and in Plexiglas parallel plates run in a constant-velocity, machine-driven system in which the pressure drop between two points on the plates was measured with a differential pressure transducer. A general method of correlating fraction laminarization or drag reduction effectiveness with polymer concentration for Reynolds numbers above 6000 was developed in which two master curves, one for very low concentrations which was the same for both tubes and parallel plates, and one for higher concentrations which differed for tubes and parallel plates, were found to represent the data very well for both polymers and all conduit sizes and Reynolds numbers. Additionally, relationships were found between conduit size and maximum fraction laminarization and optimum polymer concentration.

## INTRODUCTION

Drag reduction is the decrease of skin friction in turbulent flow due to the addition of very small amounts of certain substances to the flowing fluid. In spite of the large amount of work in the field, the basic mechanism is not yet completely understood. Wells and Spangler[1] have shown that it is a wall effect. When a drag-reducing polymer was injected into a flowing fluid at the centerline of the conduit, no drag reduction was observed until the polymer had diffused to the wall; but when the polymer was injected at the wall, the effect was immediate.

Turbulent flow is characterized by streaks or plumes of fluid which burst from the viscous sublayer creating eddies in the turbulent core of the flowing fluid.[2] These streaks, which account for 50% to 70% of the turbulent kinetic energy,[3,4] have been shown to be much more widely spaced in drag-reducing solutions[5,6,7] although of the same intensity as those in the pure solvent. Donohue[8] and Ting[9] suggest that the suppression of streaks and bursting in the viscous sublayer is a result of the polymer solution's high resistance to axisymmetic strains. Peterlin[10] has shown that the elongational viscosity, the resistance to axi-symmetric strains, is as much as four orders of magnitude greater than the shear viscosity. This is the cause of filament formation and "stringiness" in drag-reducing solutions.

TABLE I

| Tubes | | |
|---|---|---|
| Diameter $D$, cm | Length $L$, cm | $L/D$ |
| Flow System Dimensions | | |
| 0.200 | 59.8 | 299 |
| | 6.1 | 30.5 |
| 0.300 | 91.5 | 305 |
| | 9.8 | 32.7 |
| 0.476 | 91.4 | 192 |
| | 14.4 | 30.2 |
| 0.635 | 91.5 | 144 |
| | 19.4 | 30.5 |
| Parallel Plates | | |
| Spacing $b$, cm | Width $w$, cm | $w/b$ |
| 0.105 | 1.03 | 9.8 |
| 0.152 | 1.54 | 10.1 |
| 0.200 | 2.02 | 10.1 |

## EXPERIMENTAL

The object of the experiments was the determination of friction factors for flow through tubes or parallel plates. The friction factor for a given fluid and conduit depends on the velocity and pressure drop; therefore, an experiment consists of setting either one of these variables and measuring the other. Both methods were used. The tube experiments were run with a constant-head and a gravity flow system.[11] The parallel plate experiments were run with a constant-velocity and a machine-driven system.

### Tube Apparatus

A 1-liter Pyrex glass reservoir is connected to the flow tube by a 185-cm length of ½-in.-I.D. rubber tubing and a short length of ¼-in.-I.D. rubber tubing with a clamp. The reservoir is clamped to a vertical rod so that its height can be varied from zero to 200 cm above the flow tube. The flow tube is mounted horizontally, 19.6 cm above a collecting trough.

The velocity of the fluid in the tube is indicated by the horizontal distance that the effluent stream travels before hitting the top of the collecting trough. Since the stream takes 0.2 sec to fall 19.6 cm from the tube to the trough, the horizontal velocity of the stream is five times the horizontal distance traveled, measured in centimeters. The flow tubes are precision-bore, borosilicate glass tubing (Table I). Two lengths of each size flow tube are used to determine the losses due to end effects.

### Parallel-Plate Apparatus

A system using a mechanically driven piston to provide a constant velocity flow is used with the parallel plates. An aluminum cylinder and piston, sealed with a nitrile rubber O-ring, is driven at constant speed by the cross

arm of an Instron testing machine (Instron Corp., Canton, Mass.). The cylinder has an inside diameter of 4.875 in. and a capacity of about 1.5 liters. At the maximum cross-arm speed of 20 in./min, the flow rate is 102 ml/sec. A line of ½-in. copper tubing with a ⅜-in. brass ball valve connects the cylinder to the parallel plates. A line of ½-in. plastic tubing feeding into this line through a ⅜-in. brass globe valve is used to fill the cylinder. A 3/16-in. hole through the center of the piston, sealed at the top with a ¼-in. machine screw, is used to bleed air from the system.

The parallel plates, whose dimensions are given in Table I, are ¼-in. acrylic plastic with aluminum sides. Three 3/32-in. pressure taps are spaced 20 cm apart along the bottom plate. The first tap is located a distance downstream from the entrance equal to about 100 times the spacing between the plates to ensure fully developed flow. The pressure drop between any two taps is measured with a differential pressure transducer (Validyne Engineering Corp., New York, N. Y.) and carrier-demodulator reading out on a strip recorder.

To make a run, about 1 liter of solution is introduced into the cylinder through the fill tube, while the piston is being held up and the bleed hole is open. The fill valve is then closed and the piston is lowered until liquid comes out of the bleed, which is then closed. The line running from the cylinder to the plates remains full of liquid from the previous run and is not rebled.

The cross arm of the Instron machine is then lowered to the top of the piston, the main valve is opened, and the run is started at the highest speed to flush the old solution out of the lines. The speeds are selected by pushbuttons on the Instron machine, three speeds generally being run for each liter of solution. The speeds used in the turbulent region for these plates are 20, 10, and 5 in./min, corresponding to flows of 102, 51, and 25.5 ml/sec.

## Polymer Solutions

The polyacrylamide used was a partially hydrolyzed, photopolymerized sample. The intrinsic viscosity, determined in 1*N* sodium nitrate solution, was 10.2 dl/g, corresponding to a viscosity-average molecular weight of 2.1 million.[12] Test solutions were prepared by diluting about 10.5 g of the stock solution (1.9%) to 2 liters with distilled water, giving a concentration of about 100 g/m$^3$ (or ppm). One liter of this solution was used for the run and 1 liter was diluted in half to 50 g/m$^3$. The solution was successively diluted in this manner down to a concentration of about 0.20 g/m$^3$.

The poly(ethylene oxide) used was Polyox FRA (Union Carbide Corp., New York, N. Y.), supplied as a dry powder. The intrinsic viscosity, determined in water, was 7.4 dl/g, corresponding to a viscosity-average molecular weight of 1.3 million.[13] Test solutions were prepared by dissolving about 0.8 g polymer in 1 liter of distilled water by rocking for one day. This was then diluted to 2 liters and a concentration of about 400 g/m$^3$. Successive dilutions were made as with the polyacrylamide. Test solutions for both polymers were made immediately before use as both are subject to degradation in very dilute solution.

## RESULTS AND DISCUSSION

The friction factor is[14]

$$f = (\Delta pD)/(2Lu^2) \tag{1}$$

where $\Delta p$ is the pressure drop (dynes/cm$^2$) for a length $L$ (cm) of pipe with diameter $D$ (cm) in which the average velocity of fluid is $u$ (cm/sec). The Reynolds number is

$$\mathrm{Re} = Du/\nu \tag{2}$$

where $\nu$ is the kinematic viscosity in cm$^2$/sec.

The most common means of quantifying drag reduction effectiveness has been a friction factor ratio, that is, the ratio of the friction factor of the drag-reducing solution to that of the pure solvent. This is an appropriate quantity for engineering studies relating to decreases in pumping power requirements or increases in flow rates, but a better quantity for phenomenological studies is the fraction laminarization:

$$F = \frac{f_t - f}{f_t - f_1} \tag{3}$$

where $f$ is the fraction of the drag-reducing solution, $f_t$ is the friction factor of the pure solvent in turbulent flow, and $f_1$ is the theoretical friction factor of the pure solvent if it were in laminar flow at the same Reynolds number, $f_1 = 16/\mathrm{Re}$. This method is more in line with the theory that drag reduction results from the suppression of turbulence,[6-10] with laminar flow being the minimum friction situation. Whenever a conventional friction factor plot (log $f$, log Re) for a given concentration of polymer gives a straight line between the turbulent and laminar extremes with an appropriate slope, $F$ will be independent of Re. This is the case, for example, for the data of White[15] in smooth pipes. It is obviously not the case for some of the data of Hand and Williams[16] where laminar flow is extended beyond the usual transition (Re =

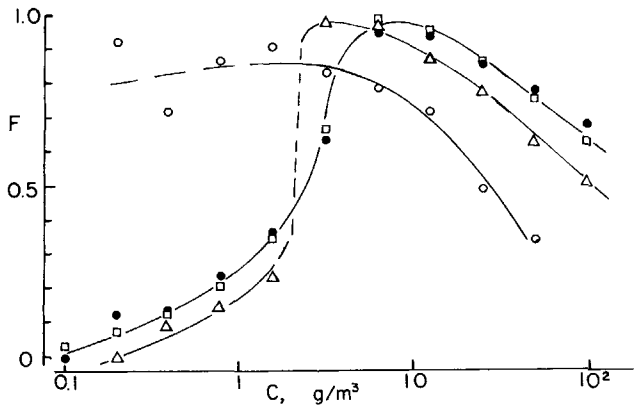


Fig. 1. Fraction laminarization $F$ vs. concentration $c$ for polyacrylamide solutions in tube with diameter = 0.300 cm; Re = 2500 (○), 3300 (△), 4200 (□), and 5000 (●).

2100) and then breaks into a region of higher friction, though still lower than the turbulent value.

At extremely high Reynolds numbers where the laminar friction factor becomes insignificant compared to the turbulent friction factor, the fraction laminarization reduces to

$$F' = 1 - \frac{f}{f_t} \tag{4}$$

and the two methods are equivalent. However, even at a Reynolds number of 20,000, the highest in this study, the laminar friction factor is still 12% of the turbulent friction factor. The fraction laminarization, under these circumstances, appears to give better correlation with other variables.

## Tubes

The behavior of fraction laminarization $F$ in tubes at various concentrations of polyacrylamide (Figs. 1 and 2) shows that above a Reynolds number of about 6000, the drag reduction effectiveness of a given concentration of polymer in a given tube becomes independent of the Reynolds number. Moreover, the change of $F$ with $N_{Re}$ at a fixed concentration $c$ is greater at high values of $c$ than at low values. In the remaining work reported here, only data for the higher Reynolds numbers are used. The ranges employed are summarized in Table II.

In order to correlate the behavior of each system, one can select any number of characteristic parameters. Those chosen here are the maximum value of $F$, $F_{max}$, and the concentration $c_0$, corresponding to that maximum. Values are listed in Table II.

When the tube diameter is increased (Fig. 3), there is a small decrease in the maximum fraction laminarization $F_{max}$. Also, there is a well-defined shift to higher "optimum" concentration $c_0$, at which $F_{max}$ and increase in $c_0$, seem more pronounced when the polymer is poly(ethylene oxide) (Fig. 4).

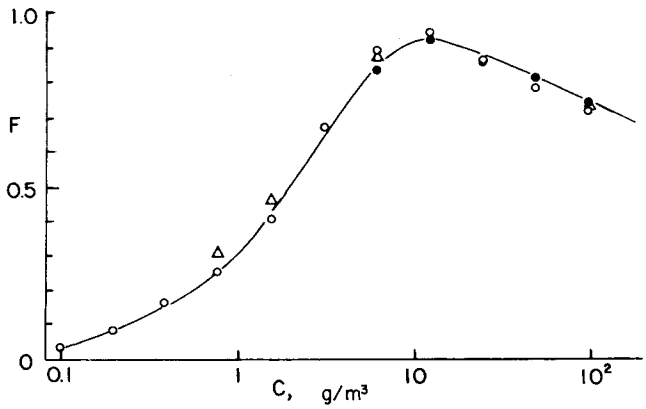


Fig. 2. Fraction laminarization as in Fig. 1: Re = 5800 (○), 6700 (△), and 8300 (●). Solid lines correspond to "master curves" of Figs. 9 and 10.

TABLE II
Drag Reduction Parameters
(PAM, Polyacrylamide, PEO, Poly(ethylene Oxide))

| Tubes | | | | | | |
|---|---|---|---|---|---|---|
| | | | | | Reynolds number Re × $10^{-3}$ | |
| $D$, cm | Polymer | $C_0$, g/m³ | $F_{max}$ | $C_2$, g/m³ | Minimum applicable | Maximum investigated |
| 0.22 | PAM | 6.1 | 1.01 | — | 4.5 | 6.1 |
| 0.300 | PAM | 12.5 | 0.93 | 0.51 | 5.8 | 9.2 |
| | PEO | 12.5 | 0.92 | 1.0 | 5.8 | 9.2 |
| 0.476 | PAM | 17 | 0.87 | 0.61 | 6.6 | 14.5 |
| | PEO | 20 | 0.91 | 1.3 | 6.6 | 14.5 |
| 0.635 | PAM | 25 | 0.85 | 0.39 | 12.3 | 19.4 |
| | PEO | 50 | 0.80 | 0.45 | 7.1 | 19.4 |

| Parallel Plates | | | | | |
|---|---|---|---|---|---|
| | | | | | Reynolds number |
| $b$, cm | Polymer | $C_0$, g/m³ | $F_{max}$ | $C_2$, g/m³ | Re × $10^{-3}$ |
| 0.105 | PAM | 30 | 0.75 | 1.3 | 10.95 |
| | PEO | 18 | 0.77 | 0.84 | 10.95 |
| 0.152 | PAM | 60 | 0.68 | 1.2 | 14.8 |
| | PEO | 100 | 0.67 | 2.1 | 14.8 |
| 0.200 | PAM | 80 | 0.64 | 1.7 | 11.2 |
| | PEO | 100 | 0.65 | 1.2 | 11.2 |

## Parallel Plates

Although the parallel-plate geometry is quite convenient for many purposes, few data have been published in recent years, even for Newtonian fluids.[17,18] At a reasonably high Reynolds number, the data for polyacrylamide (Fig. 5) and poly(ethylene oxide) (Fig. 6) in plates bear a qualitative resemblance to the data in tubes. The two trends observed in tubes, a decrease

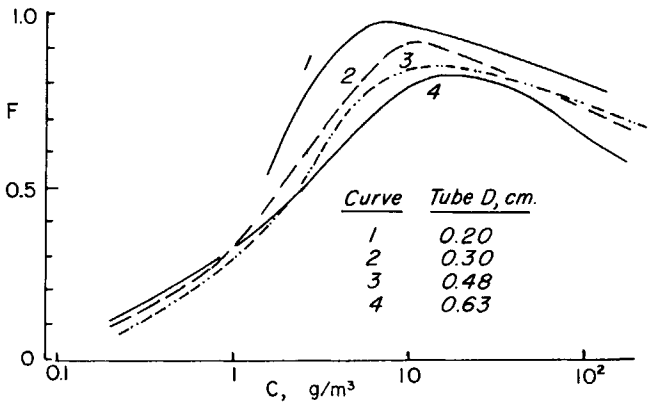


Fig. 3. Average $F$ vs. concentration for polyacrylamide solutions in four tubes at high Reynolds numbers.

in $F_{max}$ and an increase in $c_0$ with increased diameter, $D$, occur also with increasing plate spacing $b$. In comparing plates with tubes, the equivalent expression replacing $D$ in the Reynolds number is $2b$.

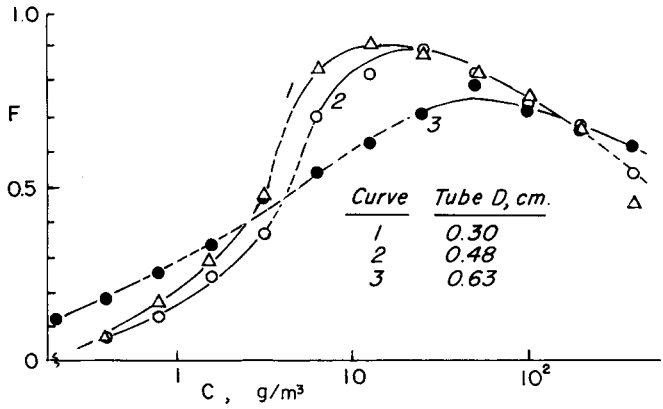


Fig. 4. Average $F$ vs. concentration for poly(ethylene oxide) solutions in three tubes at high Reynolds numbers. Solid lines correspond to "master curves" of Figs. 9 and 10.

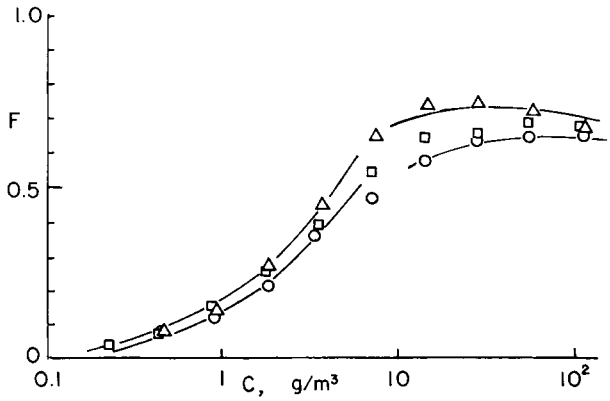


Fig. 5. Fraction laminarization for polyacrylamide solutions flowing between plates with spacing $b$; $b$ = 1.05 mm (△), 1.52 mm (□), 2.00 mm (○). Solid lines correspond to "master curves" of Figs. 9 and 10.

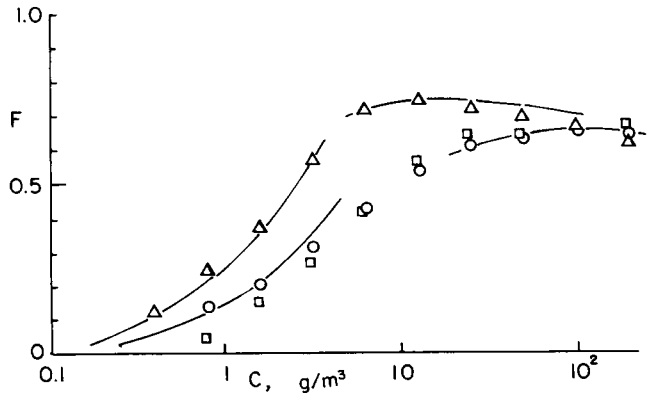


Fig. 6. Fraction laminarization for poly(ethylene oxide) solutions flowing between plates. Symbols have some significance as in Fig. 5.

The $c_0$ data for polyacrylamide and poly(ethylene oxide) were selected to be effective at about the same concentration. The data could be interpreted as showing a larger exponent, say, 2.0, for dependence of $c_0$ on $D$ or $b$ with poly(ethylene oxide), but it would be hazardous to justify an exact value on the basis of the present work. In the case of $F_{max}$, the data again more clearly support an exponential dependence on diameter for polyacrylamide than for the second polymer (Fig. 8):

Tubes:

$$F_{max} \sim D^{-0.15} \tag{6}$$

Plates:

$$F_{max} \sim b^{-0.25}. \tag{7}$$

Some idea of the success in fitting experimental data with the two constant system is indicated in Figure 9 for values of $c/c_0$ between 0.2 and 10. There is a definite difference in the shape of the curves, the data for plates showing much less change in $F/F_{max}$ with $c/c_0$ than the data for tubes.

At the low-concentration end, a second parameter is selected, $c_2$, the concentration at which $F = 0.2$. For both plates and tubes, a reasonable generalization seems possible (Fig. 10). The "master curves," that is, the solid lines in Figures 9 and 10, appear also in Figures 2, 4, 5, and 6. There appears to be no easily discerned dependence of $c_2$ on $D$ or $b$ (Fig. 11). As might be expect-

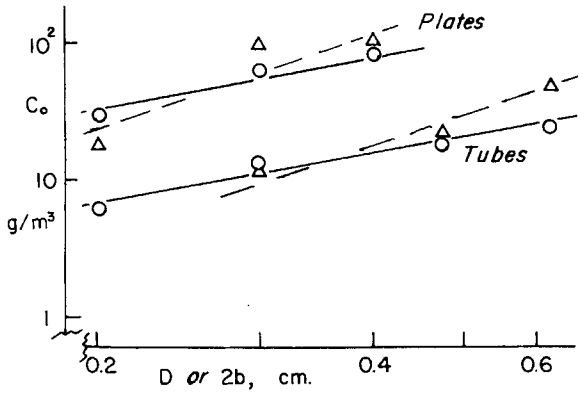


Fig. 7. Dependence of concentration at maximum laminarization $c_0$ on tube diameter $D$ or plate spacing $b$. Triangles are for poly(ethylene oxide), circles are for polyacrylamide.

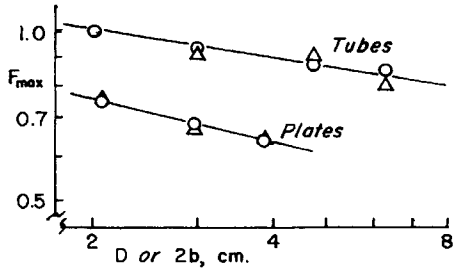


Fig. 8. Dependence of maximum laminarization $F_{max}$ on tube diameter $D$ or plate spacing $b$. Triangles are for poly(ethylene oxide), circles are for polyacrylamide.

ed, typical data points begin to deviate from superposition when $c/c_0$ exceeds about 0.3.

The same data at the low-concentration end can be treated according to the equation of Virk[19] as simplified by Little.[20,21] Using $F$ as defined by eq. (1) rather than drag reduction defined by eq. (2) as used by Little, the relationship is

$$(c/F) = ([c]/DR_m) + (c/DR_m) \tag{8}$$

where $[c]$ is the "intrinsic concentration" and $DR_m$ is interpreted to be the "maximum drag reduction." It can be shown that $[c]$ should be four times $c_2$. Assume first a value of unity for $DR_m$ in eq. (8). Then, at $F = 0.2$, $c = c_2 = [c]/4$. The smooth curve in Figure 11 corresponds to eq. (8) with $DR_m = 1$ and $[c] = 4\,c_2$. It is also possible to derive $DR_m$ from individual plots according to eq. (8). However, since they are derived from low-concentration data, often well removed from the actual maximum, it is not surprising that the values are not always realistic.

All of the fraction laminarization-versus-concentration curves seem to have the same basic shape in both the tail section at very low concentrations and the hump section around the optimum concentration. They differ only in the low-concentration fall-off region, which becomes steeper as tube diameter decreases. This suggests that the overall curve is a superposition of two curves, the tail and the hump, with the steepness of the fall-off region being

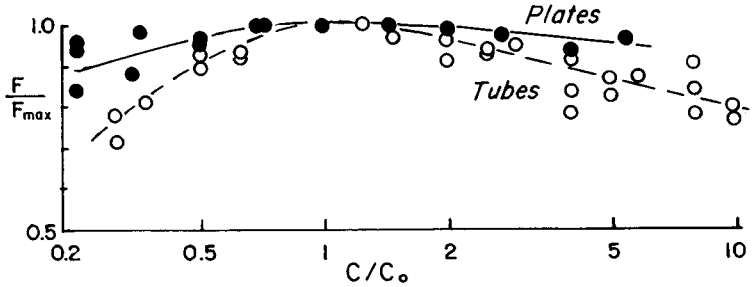


Fig. 9. Normalized fraction laminarization vs. reduced concentration in the vicinity of $c_0$.

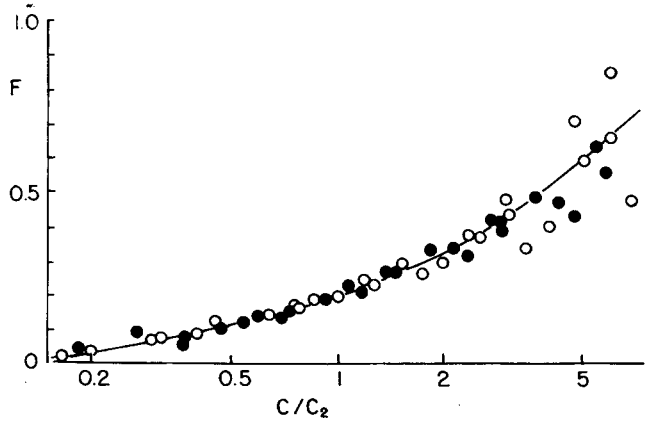


Fig. 10. Fraction laminarization vs. reduced concentration in the vicinity of $c_2$ for tubes (○) and plates (●).

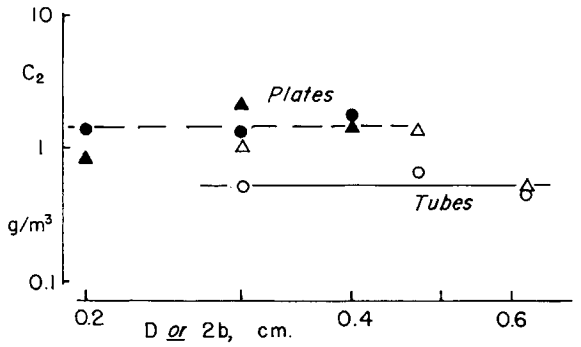


Fig. 11. Dependence of concentration at $F = 0.2$, $c_2$, on tube diameter $D$ or plate spacing $b$. Triangles are for poly(ethylene oxide), circles are for polyacrylamide.

determined by the point at which the two curves intersect. The reality of these two sections, the tail and the hump, suggests further that there may be also two separate effects in the drag reduction mechanism depending on concentration of polymer.

In the hump section of the curve, the polymer is at a high enough concentration that the molecules do not act independently. The molecular entanglements may cause a thickening of the viscous sublayer, with the resulting decrease in the generation of turbulent eddies discussed in the introduction.

At the low concentrations in the tail section of the curve, the polymer molecules probably act independently, and a small amount of drag reduction produced may be the result of the interference of individual molecules with the energy dissipation process in turbulent eddies. Peterlin[22] suggests that a macromolecular coil encountering the large velocity gradient between an eddy and the surrounding fluid is deformed and that the resulting expanded coil produces a larger local relative viscosity tending to damp out the eddy.

Both effects, the modification of the viscous sublayer and the interference with the eddies, occur at higher concentrations, leading to the superposition of the two curves. The wall effect predominates in the vicinity of the optimum concentration because up to 70% of the turbulent kinetic energy is contained in the streaks and bursts from the viscous sublayer.[3,4] These effects may also explain the steeper transition between tail and hump for the smaller conduits. In a small conduit, the area near the wall is a larger fraction of the total area; therefore, the wall effect becomes an important part of the total effect at a lower concentration.

## References

1. C. S. Wells and J. G. Spangler, *Phys. Fluids*, **10**, 1890 (1967).
2. E. R. Corino and R. S. Brodkey, *J. Fluid Mech.*, **37**, 1 (1969).
3. S. J. Kline, H. T. Kim, and W. C. Reynolds, *J. Fluid Mech.*, **50**, 133 (1971).
4. J. M. Wallace, H. Eckelmann, and R. S. Brodkey, *J. Fluid Mech.*, **54**, 39 (1972).
5. G. Fortuna and T. J. Hanratty, *J. Fluid Mech.*, **53**, 575 (1972).
6. L. D. Eckelmann, G. Fortuna, and T. J. Hanratty, *Nature*, **236**, 94 (1972).
7. R. J. Gordon, *Nature*, **227**, 599 (1970).
8. G. L. Donohue, W. G. Tiederman, and M. M. Reischman, *J. Fluid Mech.*, **56**, 559 (1972).

9. R. Y. Ting, *J. Appl. Polym. Sci.*, **16,** 3169 (1972).
10. A. Peterlin, *J. Polym. Sci. 8,* **4,** 287 (1966).
11. F. Rodriguez, *Nature, Phys. Sci.* **230,** 152 (1971).
12. W. Scholtan, *Makromol. Chem.*, **14,** 169 (1954).
13. F. E. Bailey, Jr., J. L. Kucera, and L. G. Imhof, *J. Polym. Sci.*, **32,** 517 (1958).
14. C. O. Bennett and J. E. Myers, *Momentum, Mass, and Heat Transfer,* 2nd ed., McGraw-Hill, New York, 1974, pp. 17, 164.
15. W. D. White, in *Viscous Drag Reduction,* C. Sinclair Wells, Ed., Plenum Press, New York, 1969, pp. 173.
16. J. H. Hand and M. C. Williams, *Nature,* **227,** 369 (1970).
17. R. R. Rothfus, R. I. Kermode, and J. H. Hackworth, *Chem. Eng.*, **71,** (25) 175 (1964).
18. R. W. Hanks and H.-C. Ruo, *Ind. Eng. Chem., Fundam.*, **5,** 558 (1966).
19. P. S. Virk, E. W. Merrill, H. S. Mickley, K. A. Smith, and E. L. Mollo-Christensen, *J. Fluid Mech.*, **30,** 305 (1967).
20. R.C. Little, *J. Colloid Interfac. Sci.*, **37,** 811 (1971).
21. R. Y. Ting and R. C. Little, *J. Appl. Polym. Sci.*, **17,** 3345 (1973).
22. A. Peterlin, *Nature,* **227,** 598 (1970).

Received June 11, 1975
Revised June 23, 1975